

Investigation of ion transport in ohmic discharges by charge-exchange recombination spectroscopy with a diagnostic hydrogen beam in TEXTOR-94

A. Kreter¹, R. Jaspers², A. Krämer-Flecken¹, B. Schweer¹,
M. Z. Tokar¹, B. Unterberg¹

Partners in the Trilateral Euregio Cluster:

¹*Institut für Plasmaphysik, Forschungszentrum Jülich GmbH, EURATOM Association,
52425 Jülich, Germany*

²*FOM Instituut voor Plasmafysica Rijnhuizen, EURATOM Association,
Postbus 1207, 3430 BE Nieuwegein, The Netherlands*

1. Introduction

In addition to the two heating neutral beam injectors routinely used for the Charge-eXchange Recombination Spectroscopy (CXRS) [1] a novel diagnostic hydrogen beam has recently been installed at the tokamak TEXTOR-94. With the new beam measurements of the ion temperature and impurity density under all discharge conditions with an improved radial resolution became possible. A detailed description of the diagnostic injector and experimental set-up is given in section 2.

First CX measurements at TEXTOR-94 in ohmic discharges were performed at different plasma densities and plasma currents. The ion transport properties in the ohmic regime were deduced from the ion temperature profiles measured with the diagnostic beam. A rise of the temperature in the inner half of the minor radius of both ions and electrons was observed in high density discharges during the transition from Saturated Ohmic Confinement (SOC) to Improved Ohmic Confinement (IOC). The ratio η_i of plasma density and ion temperature decay lengths at half the minor radius is lower for the IOC case. This indicates a reduction of the anomalous transport caused by the ion temperature gradient (ITG) driven instability. The development of the plasma properties and the ITG instability growth rate during the SOC – IOC transition is discussed in section 3.

2. Diagnostic neutral beam injector

RUDI (RUSSIAN Diagnostic Injector) is based on a RF-discharge ion source developed in the Budker Institute of Nuclear Physics Novosibirsk, Russia, which provides an equivalent neutral current of 1 A with an extracting voltage of 20-50 kV [2]. Together with a small angle divergence of ± 0.5 degree it leads, on the one hand, to a beam current density for sufficiently high charge-exchange signals; on the other hand, the heating power and plasma dilution are negligible, so that measurements with the pure ohmic or RF heating are also possible. A RUDI pulse duration of currently up to 4 seconds allows measurements of the ion temperature and impurity densities during almost the whole TEXTOR-94 discharge with an easy distinction between active CX signal and passive background due to the modulation of the beam. An overview on the beam parameters is given in table 1.

Figure 1 shows the general layout of the diagnostic injector at TEXTOR-94. The cold plasma is produced in the RF driven plasma generator. Ions are extracted from the RF plasma box and accelerated by the four grids ion optical system. To provide a neutral beam, the ions are neutralized by charge exchange with the gas target. The neutral beam passes through the vacuum tank and beam line into the plasma. Inside the vacuum tank a bending magnet is installed to separate the remaining ions from the neutral beam particles. A retractable segmented calorimeter installed in the beam line is used for the measurements of the beam profile.

Table 1. Characteristics of the diagnostic neutral beam injector RUDI at TEXTOR-94

Beam energy	20-50 keV
Ion / neutral beam current	1.8 A / 1 A
Operated / max. pulse length	4 s / 10 s
Modulation frequency	500 Hz
Ion species mix ($H^+ : H_2^+ : H_3^+$)	50 : 20 : 30
1/e beam width in 4.1 m / beam divergence	80 mm / $\pm 0.5^\circ$
Max. neutral beam current density in 4.1 m	17 mA/cm ²

The vacuum system consisting of a rotary pump, roots blower and turbo-molecular pump is used for the initial pump down of the injector vessel. Additionally two efficient cryogenic pumps are installed in the vacuum tank to prevent the reionization of the beam particles and plasma dilution with hydrogen during the operation.

The observation system covers the whole beam path in the plasma. There are three windows available: for the high field side, central and edge plasma observation. The two latter ports, which are currently used, provide the observation from the edge to the center with a radial resolution of 1.5 cm at the edge and about 5 cm in the center, determined by the beam width. The time resolution is limited by the detector frame rate of 20 fps. For this reason, the beam is usually operated in a so-called supermodulation regime with a frequency of 10 Hz.

3. Transport studies in ohmic discharges

The ion temperature measurements presented below were done using CXRS at the carbon line CVI at 529.0 nm. The ratio of active and passive components of the CX signal varies between 1:2 in case of ohmically heated discharges at a medium plasma density and 1:10 in high density discharges with additional heating.

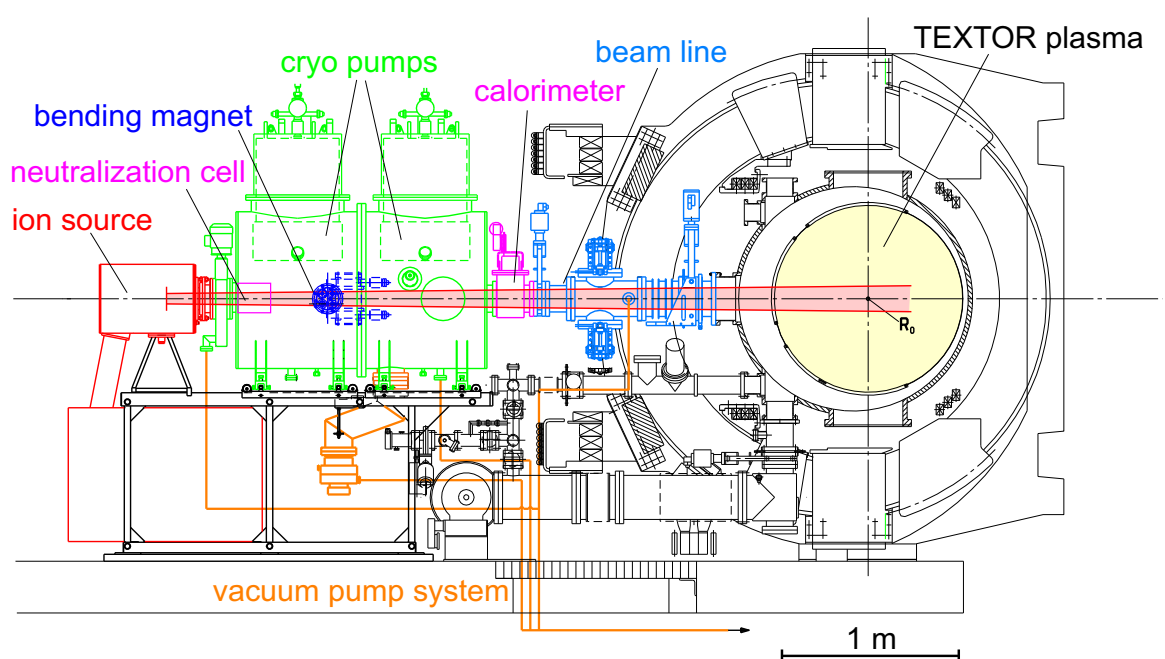


Figure 1. Set-up of the diagnostic neutral beam injector RUDI at TEXTOR-94.

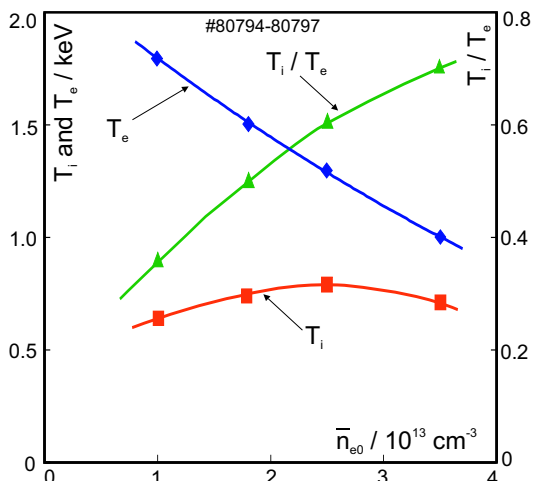


Figure 2. Density scan in ohmic discharges ($I_p = 350$ kA, $P_{OH} = 300$ kW). Ion temperature was measured with RUDI, electron temperature with the ECE diagnostic, $R-R_0 = 5$ cm.

A comprehensive study of the influence of the plasma density on the central ion and electron temperature under ohmic conditions has been made. The electron temperature T_e was measured by the ECE diagnostics. In ohmic discharges the electrons are primarily heated, whereas the ions are heated only via collisions with electrons. Obviously, the energy transfer from electrons to ions is larger for higher densities leading to an increase of T_{i0}/T_{e0} from 0.4 to almost unity (fig. 2). Therefore, although T_{e0} decreases with the rising density, T_{i0} first increases, reaches a maximum at $\bar{n}_{e0} \approx 2.5 \cdot 10^{13} \text{ cm}^{-3}$ and then decreases together with T_{e0} .

One characteristic feature of the ohmic confinement at low densities is the linear dependence of the energy confinement time on the plasma density, the so-called Linear Ohmic Confinement (LOC). However, at higher densities the confinement becomes almost independent of plasma density (SOC – Saturated Ohmic Confinement). This fact is clearly seen in the behaviour of the diamagnetic energy E_{dia} during a density ramp (fig. 3). The energy increases linearly with the rising density before it saturates. When at densities close to the density limit the external gas feed is switched off, like it was done in this discharge, E_{dia} jumps to a higher value for the same density, indicating a transition from saturated to Improved Ohmic Confinement (IOC [3]). The improvement is seen in both electron and ion channels. The SOC – IOC transition shows many similarities to the transition from L-mode to the so-called Radiative Improved mode (RI-mode) [4]. In fact, the normalized confinement time of L-mode / SOC and RI-mode / IOC scales equivalently with the normalized plasma density. The L – RI transition was successfully described by a model based on the suppression of the Ion Temperature Gradient (ITG) driven instability due to the presence of impurities and the peaking of the density in the RI-mode [5]. One characteristic parameter for the ITG instability is the ratio η_i of plasma density and ion temperature decay lengths. Lower values of η_i indicate a reduction of the ITG mode. For the SOC – IOC transition we analyzed the temperature and density profiles and calculated the η_i profile for the time points just before and after the transition. The profile peaking in the IOC regime is clearly seen in both electron and ion temperature profiles as well as in the density profile (fig. 4). In the radial region close to half the minor radius, where the profile gradients are the largest, the η_i values for the IOC

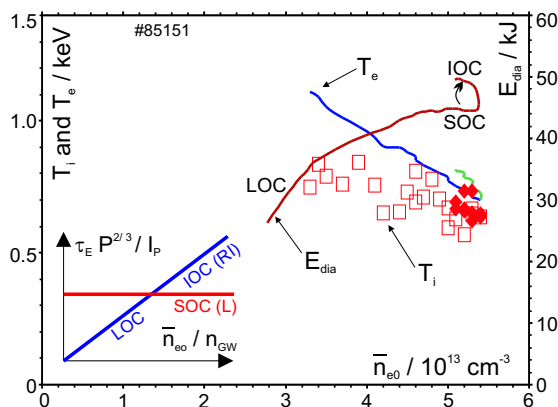


Figure 3. Diamagnetic energy, ion and electron temperatures as functions of the central line averaged electron density in an ohmic discharge ($I_p = 400$ kA, $P_{OH} = 450$ kW). After the density ramp was stopped by switching off the external gas feed, a clear SOC-IOC transition was seen. In the insert a schematic representation of the normalized confinement time as a function of the density for ohmic (LOC, SOC, IOC) and additionally heated discharges (L, RI) is shown (cf. [4]).

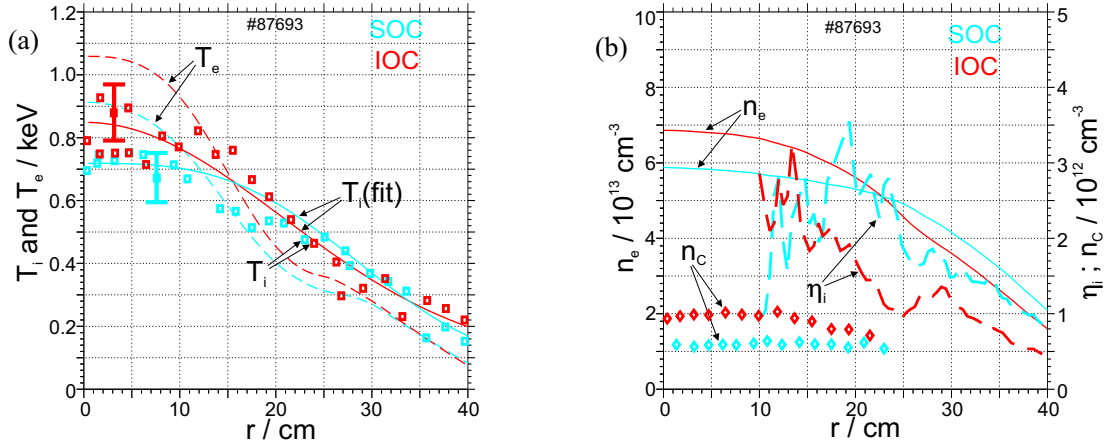


Figure 4. Profiles before (blue) and after (red) SOC – IOC transition. (a) boxes – ion temperature, solid lines – fit functions used for calculations, broken lines – electron temperature; (b) solid lines – electron density, diamonds – density of fully stripped carbon, broken lines – calculated η_i profiles.

case are considerably lower, indicating the suppression of the ITG mode. Using now the radial profiles of the ion and electron temperature as well as of the electron density and of the density of fully stripped carbon, which is the dominant impurity species in the ohmic plasmas, the spectrum of the toroidal ITG growth rate can be calculated [6]. We obtain at half the minor radius a considerable reduction of the ITG growth rate over the whole spectrum of the wave number k_θ (fig. 5).

4. Conclusions and outlook

The novel diagnostic hydrogen beam RUDI is an enhancement of the CXRS measurement at TEXTOR-94 facilitating measurements of the ion temperature and impurity densities under all discharge conditions with an improved radial resolution.

The ion transport properties in the ohmic regime were investigated using the ion temperature profiles measured with the diagnostic beam. The analysis of the profiles at the SOC – IOC transition shows a reduction of the toroidal ITG instability.

In the future the signal to noise ratio of the CX signal will be improved in order to reduce the uncertainty of the measured parameters in high density discharges with additional heating. This can be achieved by increasing the beam current as well as by improvement of the beam species distribution. A new high speed CCD detector, which can follow the 500 Hz beam modulation, will not only improve the time resolution of the measurements but also increase the ration of active to passive component of the CX signal.

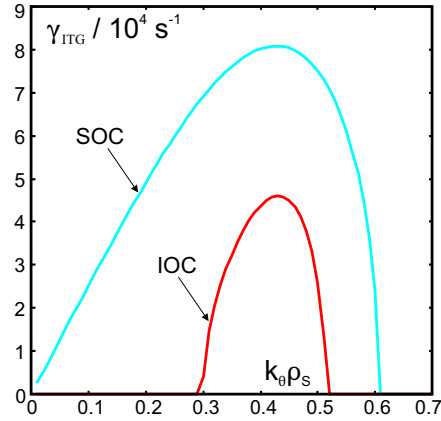


Figure 5. ITG instability growth rate γ_{ITG} as a function of the dimensionless poloidal wave vector at $r/a = 0.5$ (ρ_s is the Larmor radius of deuterons).

- [1] E. Busche, H. Euringer, R. Jaspers, Plasma Phys. Control. Fusion **39** (1997) 1327.
- [2] A. A. Ivanov et al., Transactions of Fusion Technology **35** (1999) 180.
- [3] F. X. Söldner, E. R. Müller, F. Wagner et al., Phys. Rev. Lett. **61** (1988) 1105.
- [4] R. Weynants et al., Nucl. Fusion **39** (1999) 1637.
- [5] M. Z. Tokar, J. Ongena, B. Unterberg, R. R. Weynants, Phys. Rev. Lett. **84** (2000) 895.
- [6] M. Z. Tokar et al., Plasma Phys. Control. Fusion **41** (1999) L9.